

Coupling-driven transition from multiple to single-dot interference in open quantum-dot arraysM. Elhassan,¹ J. P. Bird,¹ A. Shailos,¹ C. Prasad,¹ R. Akis,¹ D. K. Ferry,¹ Y. Takagaki,² L.-H. Lin,³ N. Aoki,³ Y. Ochiai,³ K. Ishibashi,⁴ and Y. Aoyagi⁴¹*Department of Electrical Engineering and Center for Solid State Electronics Research, Arizona State University, Tempe, Arizona 85287-5706*²*Paul-Drude-Institut für Festkörperelektronik, Hausvogteiplatz 5-7, D-10117 Berlin, Germany*³*Department of Materials Technology, Chiba University, 1-33 Yayoi-cho, Inage-ku, Chiba 236-8522, Japan*⁴*The Institute for Physical and Chemical Research (RIKEN), 2-1 Hirosawa, Wako-shi, Saitama 351-0198, Japan*

(Received 23 April 2001; published 8 August 2001)

The details of electron interference in open quantum-dot arrays are studied in experiment and numerical simulations. Reproducible fluctuations are observed in their low-temperature magnetoconductance and the characteristics of these are suggested to be consistent with a transition from multiple to single-dot interference, which occurs as the strength of the interdot coupling is varied. These results therefore reveal a nontrivial scaling of the conductance fluctuations in quantum-dot arrays, which is thought to arise due to the influence of the interdot coupling on energy hybridization.

DOI: 10.1103/PhysRevB.64.085325

PACS number(s): 73.23.Ad, 72.20.-i, 85.35.Be

I. INTRODUCTION

The electrical properties of quantum dots are known to be strongly influenced by electron interference, an effect that is responsible for the observation of reproducible fluctuations in their magnetoconductance.¹⁻¹⁶ In a semiclassical interpretation, the fluctuations are understood to result when the magnetic field modulates the total phase of electron partial waves trapped within the dot.¹ The fluctuations may equivalently be viewed as arising, however, when the magnetic field sweeps the discrete states of the dot past the Fermi level.^{5,8,12-15} With the dot coupled to its reservoirs by means of multimode quantum point contacts, its eigenstates develop a nonuniform broadening,¹⁵ and the fluctuations can be associated with those few states that persist in the presence of this coupling.¹³ The fluctuations provide a powerful experimental tool for the study of quantum chaos, and have been used in recent years to investigate signatures of random-matrix theory,⁴ wave-function scarring,^{7,12} and phase-space dynamics.^{9,10} For a recent overview of these studies we refer the interested reader to Ref. 16.

While the details of electron interference in open quantum dots are well understood, few studies to date have considered how this interference is modified when several dots are coupled to each other.¹⁷ In this report, we therefore investigate the factors that influence electron interference in open systems of coupled quantum-dot arrays, by studying the characteristics of the interference-related fluctuations observed in their low-temperature magnetoconductance. The quantum-dot arrays are realized in high-mobility heterojunction material, and the magnitude of the fluctuations observed in their magnetoconductance is found to approach e^2/h at low temperatures, indicating the *highly coherent* nature of transport within the arrays. We focus here on the results of experimental studies of the influence of the split-gate voltage on the frequency content of these fluctuations. Our main observation is a suppression of the high-frequency content of the fluctuations, which we observe as the gate voltage is made increasingly negative. Such behavior is shown to be

very different to that exhibited in similar studies of individual quantum dots, which leads us to suggest that it results from a transition at multiple to single-dot interference, which occurs as the strength of the interdot coupling is varied. Similar behavior is also found in realistic simulations of the arrays, which reveal an unexpected scaling of the conductance fluctuations in these structures. An important finding of our studies is that the nature of interference in coupled quantum dots can be critically determined by the strength of the interdot coupling, and we discuss this result in terms of the influence of the coupling on energy hybridization¹⁷⁻²³ in the arrays.

The organization of this report is as follows. In the following section, we describe the basic details of the fabrication, and low-temperature characterization, of the split-gate quantum-dot arrays. Our main experimental results are then presented in Sec. III, and are followed by the result of our numerical simulations in Sec. IV. Our final conclusions are presented in Sec. V.

II. DEVICE FABRICATION AND BASIC CHARACTERIZATION

Split-gate quantum-dot arrays, consisting of three identical dots connected in series, were formed in the two-dimensional electron gas of a GaAs/AlGaAs heterojunction²⁴ (Fig. 1, left inset). Results from two arrays are presented here, whose dots had lithographic dimensions of $0.6 \times 1.0 \mu\text{m}^2$ and $0.4 \times 0.7 \mu\text{m}^2$. The sample was mounted in a dilution refrigerator and measurements at 1.7 K revealed that the two-dimensional electron gas had a carrier density of $3.8 \times 10^{11} \text{cm}^{-2}$ and a mobility of $1.2 \times 10^6 \text{cm}^2/\text{Vs}$, from which we infer a transport mean-free path of at least $12 \mu\text{m}$. This value is several times larger than the total length of the arrays that we study. Unless stated otherwise, the magnetoconductance measurements we present here were made at a cryostat temperature of 10 mK, using a longitudinal four-probe configuration. Standard lock-in techniques were employed for these measurements, which were performed at a

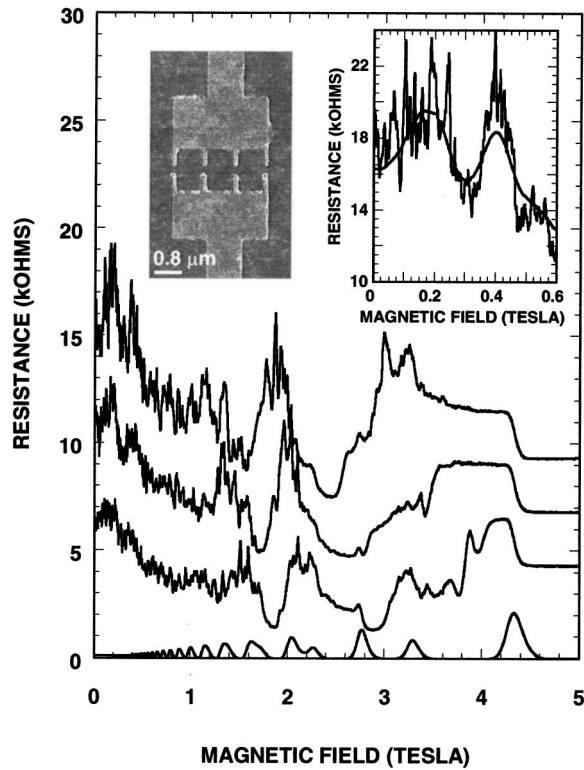


FIG. 1. The gate-voltage-dependent evolution of the magnetoresistance of the array with dot dimensions of $0.6 \times 1.0 \mu\text{m}^2$. From bottom to top, the different curves were obtained for gate voltages of 0 V, -0.64 V, -0.74 V, and -0.82 V, respectively. The left inset shows a scanning electron micrograph of an array with a similar geometry to that studied here. The right inset illustrates the temperature dependence of the magnetoresistance. The fluctuating curve was obtained at 0.05 K, while the smooth one was obtained at 4 K. The gate voltage was -1.08 V for both curves.

frequency of 11 Hz using a constant current of 0.5 nA.

In Fig. 1, we illustrate the gate-voltage-dependent evolution of the magnetoresistance of one of the arrays. Generic features here include the observation of reproducible fluctuations at low magnetic fields (<1 T), and the emergence of quantum-Hall plateaus at much higher fields (>3 T). An analysis of the evolution of the fluctuations, between the low-field and quantum-Hall regimes, allows an estimate for the phase-breaking time of the electrons to be obtained,¹¹ and for the arrays we study here a typical value of 100 ps is obtained for this parameter at base temperature. Importantly, we note that, during this long time interval, electrons trapped within the arrays may travel a total distance of $27 \mu\text{m}$ before losing phase coherence. Since this distance is very much longer than the maximum lithographic length of the arrays, we expect the details of electron transport within them to be strongly influenced by the details of the interdot coupling. Finally, we point out that the measurements presented here were obtained under conditions where the average conductance of the arrays ranged from $\sim 1 - 8e^2/h$. (At any gate voltage, we define the average conductance as the experimentally measured value at a temperature of 3 K, in the absence of an applied magnetic field. At this elevated temperature, any transport features due to interference are

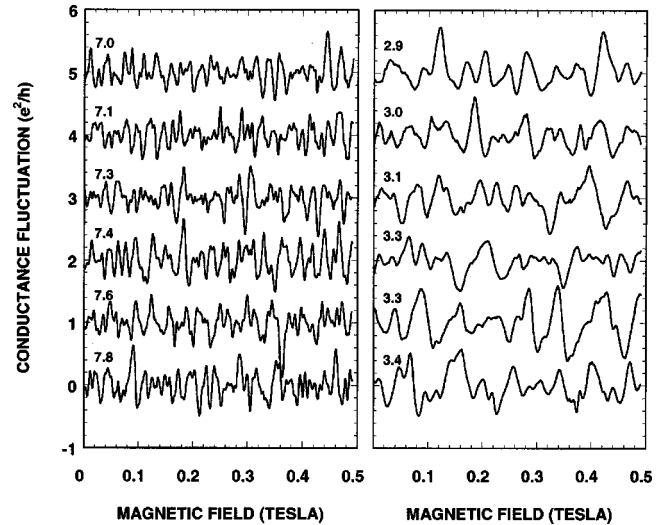


FIG. 2. Conductance fluctuations measured in an array with dot dimensions of $0.4 \times 0.7 \mu\text{m}^2$. Successive curves differ by a gate-voltage increment of 10 mV and are shifted upwards by e^2/h for clarity. The gate voltage ranged from -0.61 to -0.66 V in the left-hand panel and from -1.04 to -1.09 V in the right-hand one. The average conductance in e^2/h is indicated by the numbers on the left-hand side of each plot.

washed out completely and the average conductance should be limited by the quantum-point-contact transmissions.) Consequently, we expect that the Coulomb blockade should be suppressed and that the transport studies should allow an unambiguous probe of interference effects in the arrays.

III. EXPERIMENTAL RESULTS

Our interest in this report lies in studying the influence of the split-gate voltage on the characteristic features of the magnetoconductance fluctuations observed in the arrays. These fluctuations disappear on increasing the temperature to a few degrees Kelvin (Fig. 1, right inset), indicating that their origin lies in a coherent interference effect. In Fig. 2, we show examples of these fluctuations on an expanded magnetic-field scale. These fluctuations were obtained by subtracting a slowly varying background from the raw magnetoconductance data. The choice of this background is motivated by proper physical considerations, as we illustrate in the right-hand inset to Fig. 1. As this figure shows, at a temperature of 4 K, the fluctuations are washed out completely but an oscillating background remains. Although not shown here, these slower oscillations persist with only a weakly reduced amplitude to temperatures higher than 7 K, suggesting that they result from a classical magnetofocusing effect.^{16,25} To subtract these oscillations from the raw data, we simply mimic the low-frequency magnetoconductance variation with an appropriate polynomial fit. (While the specific choice of this background may affect the low-frequency components of the fluctuations, it will have little influence on the high-frequency components, whose characteristics we will be concerned with for an analysis in this report.)

Returning to the data presented in Fig. 2, the left-hand plot shows the fluctuations obtained at six closely spaced

gate voltages for which the average conductance of the array was close to $7 e^2/h$. The right-hand plot, on the other hand, was obtained for an average conductance close to $3 e^2/h$, and the first feature of these two plots that we notice is the large amplitude of the conductance fluctuations. In all cases shown, these are roughly of order e^2/h in magnitude, indicating that transport remains coherent in spite of the strong coupling that exists between the three dots. The other important feature of Fig. 2 is a marked suppression of the high-frequency content of the fluctuations, which arises as we make the gate voltage more negative and so reduce the average conductance. This can also be seen in the upper two panels of Fig. 3, in which we use color contours to plot the gate-voltage-dependent evolution of the fluctuation, Fourier spectra of the two arrays. (These contours were constructed from measurements performed at 50, equally spaced, gate voltages in each array.) As the gate voltage is made more negative, a damping of the high-frequency features in the contours occurs, which is consistent with the evolution shown earlier in Fig. 2.

We emphasize that the behavior shown in Figs. 2 and 3 is very different to that found in our previous studies of *individual* quantum dots, in which we typically find that the frequency content of the fluctuations is largely insensitive to changes in the gate voltage. In Fig. 4, for example, we show the conductance fluctuations measured in a single dot for a wide range of its average conductance. The dot is lithographically square, with a linear gate dimension of $0.4 \mu\text{m}$ (for further details see Ref. 6), and it is clear from Fig. 4 that the frequency content of its fluctuations is not significantly altered as the dot conductance is varied over a wide range. This in turn leads us to suggest that it is the influence of the gate voltage on the *interdot coupling* that is responsible for the behavior we observe in the arrays. To further explore this possibility, in the following section we present the results of realistic numerical simulations of quantum transport in the arrays.

IV. NUMERICAL SIMULATIONS

To simulate the behavior found in experiment, we begin by using a Poisson solver to compute the potential profile of the arrays at a series of closely spaced gate voltages. The solver uses the wafer parameters as inputs and reproduces closely the pinch-off characteristics of the arrays. Here we present results obtained for an array whose component dots have lithographic dimensions of $0.4 \times 0.7 \mu\text{m}^2$ and examples of the computed profiles are illustrated in Fig. 5. At each gate voltage, the conductance is computed as a function of magnetic field and energy, using a lattice discretization of the Schrödinger equation. The role of the interdot coupling is naturally included in the simulations, which use the computed profile of the open arrays in the lattice discretization. The finite phase-breaking time of the electrons is accounted for in the simulations by adding to the Hamiltonian an imaginary potential ($V_{im} = \hbar\hbar/2\tau_\phi$) that is chosen to match the values of τ_ϕ inferred from experiment. Further details on these calculational approaches are provided elsewhere.^{7,12,26,27}

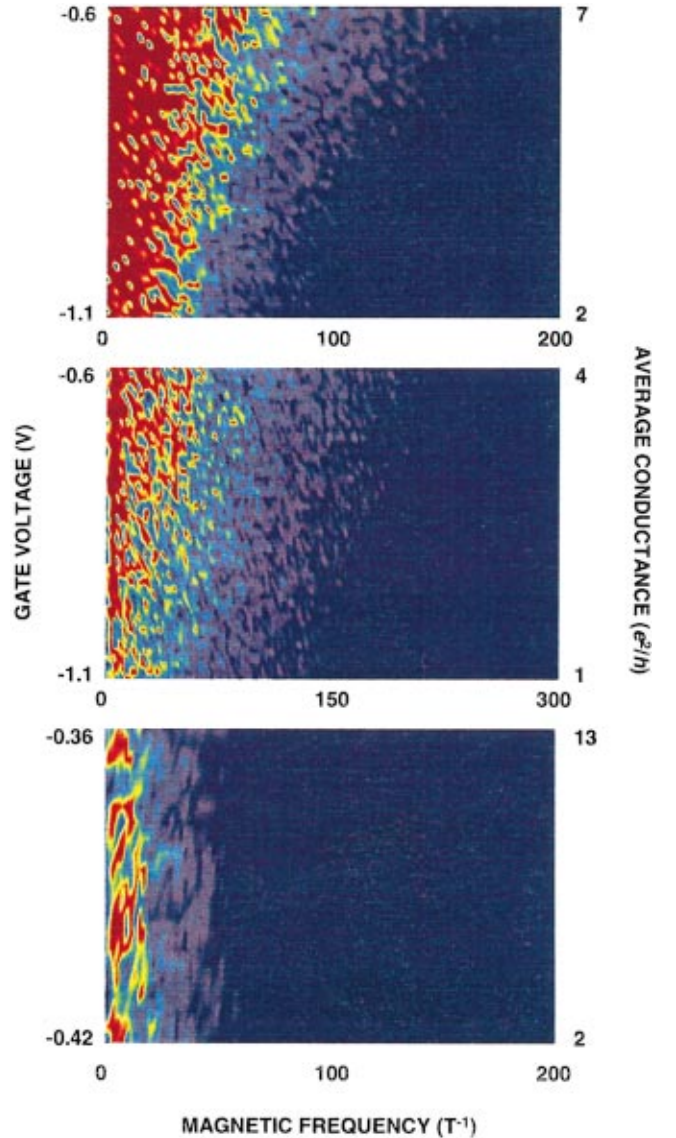


FIG. 3. (Color) Upper panel: Fourier contour plot constructed from the results of 50 magnetoresistance measurements of the array with dot dimensions of $0.4 \times 0.7 \mu\text{m}^2$. The gate voltage was incremented by 10 mV between successive measurements. Center panel: Fourier contour plot constructed from the results of 50 magnetoresistance measurements of the array with dot dimensions of $0.6 \times 1.0 \mu\text{m}^2$. The gate voltage was incremented by 10 mV between successive measurements. Bottom panel: Fourier contour plot constructed from the results of 25 magnetoresistance measurements of a $0.4\text{-}\mu\text{m}$ lithographically square dot. The gate voltage was incremented nonuniformly between successive measurements. In all three panels, a color variation from blue to red corresponds to a change in Fourier amplitude from 5 to 70, respectively.

To establish the connection between the conductance of the arrays and their density of states, in Fig. 6 we plot the variation of their conductance fluctuations in the energy-magnetic-field plane. Each of these conductance contours was obtained by computing the variation of conductance with magnetic field at 40 equidistant energies in the range from 15.15 to 15.30 meV. The choice of this energy range is not significant, although it is close to the experimentally de-

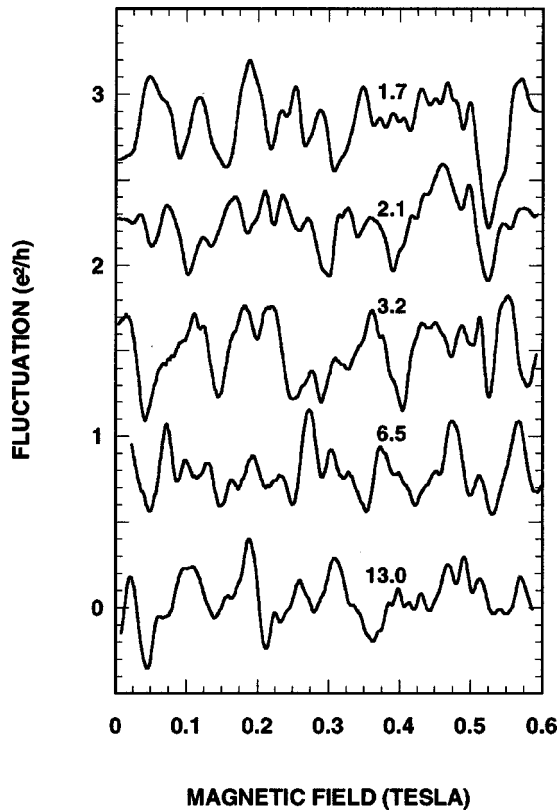


FIG. 4. Conductance fluctuations measured in a *single* dot with a lithographic size of $0.4 \mu\text{m}$ (see Ref. 6 for further details). Successive traces are offset by $0.75 e^2/h$ for clarity. The average conductance is indicated by the number associated with each data trace.

terminated Fermi energy (14 meV). The resulting grayscale plots shown in Fig. 6 were each obtained assuming a fixed gate voltage, and indicate the conductance modulation that results when the magnetic field and/or the Fermi energy are varied. In previous studies of single dots, such conductance contours have been found to be intimately related to the de-

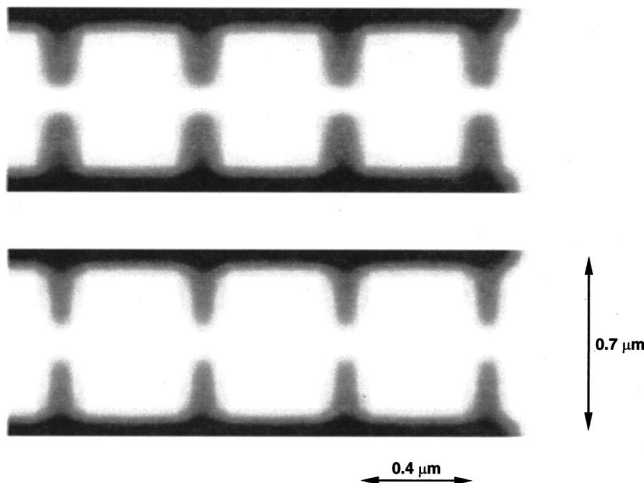


FIG. 5. The self-consistently computed potential profiles of the dot-array system that we model. The upper profile was obtained assuming a gate voltage of -0.9 V , while the lower one was obtained for a gate voltage of -0.6 V .

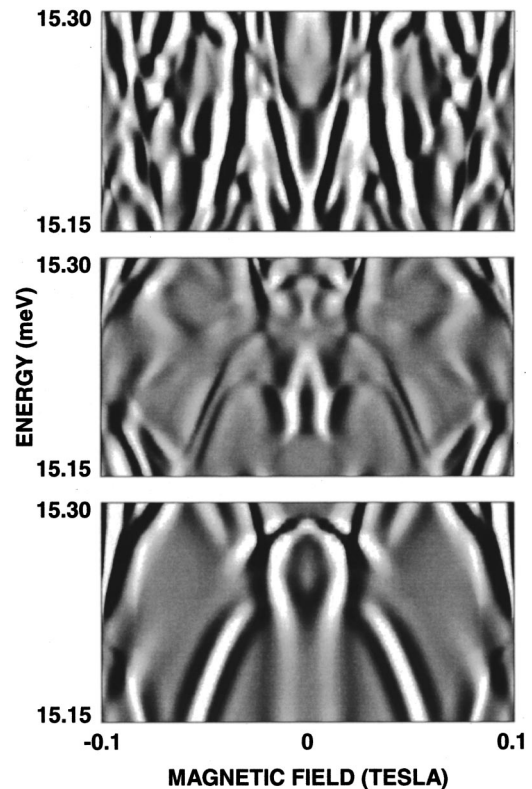


FIG. 6. Conductance contour plots for a three-dot array with lithographic dot dimensions of $0.6 \times 1.0 \mu\text{m}^2$ and a gate voltage of -0.6 V (upper panel), the same array at a gate voltage of -0.9 V (middle panel), and a single dot of dimensions $0.6 \times 1.0 \mu\text{m}^2$ and a gate voltage of -0.9 V (lower panel). Note that conductance *fluctuations* are plotted in this figure and were obtained by subtracting the average conductance from the raw data. The color variation from black to white corresponds to a conductance variation from $-0.1 e^2/h$ to $0.2 e^2/h$ in all three plots.

tails of the density of states, with the strongly striated features that run through the contours being found to follow the evolution of specific eigenstates in the magnetic field.^{13,14} As was mentioned already in the introduction, opening the dot to its external reservoirs by means of quantum-point-contact leads gives rise to a nonuniform broadening of its discrete states. For the purpose of the discussion here, the important point to note is that a variation of the magnetic field in experiment may be used to sweep this density of states past the Fermi level, giving rise to the resulting fluctuations in the magnetoconductance.¹³

The conductance contours plotted in Fig. 6 were obtained for the dot-array system of Fig. 5, and for a single dot whose lithographic dimensions were taken to be identical to those of the component dots that form the array. In the uppermost panel of Fig. 6, we show the conductance contour for the dot array, with a voltage of -0.6 V applied to its defining gates. The center panel was obtained for this same array, but this time with a gate voltage of -0.9 V , corresponding to the case of weaker interdot coupling (compare the potential profiles plotted in Fig. 5). Finally, the lower panel of Fig. 6 was obtained for the single dot, with a gate voltage of -0.9 V . From a comparison of the features plotted in the upper two panels, it is clear that the high-frequency structure in the magnetoconductance of the arrays becomes suppressed when

the gate voltage is made more negative. This is quite consistent with the behavior that we observe in experiment, as illustrated in Fig. 2, and in the upper two panels of Fig. 3. Quite surprisingly, however, from a comparison of the behavior in the lower two panels of Fig. 6, we see that the features exhibited by the array *resemble very closely those that are found for the single dot*. That is, increasing the negative gate voltage applied to the array appears to induce a transition from multiple dot to single-dot-like interference.

V. DISCUSSION AND CONCLUSIONS

Given the connection that the conductance contours provide to the density of states, the differences apparent in the upper two panels of Fig. 6 indicate that the level spectrum within the arrays develops a *finer* structure as the gate voltage is made *less* negative. We believe that this effect results from the influence of the interdot coupling on hybridization^{17–23} of the density of states in the arrays. As we demonstrate below, the main effect of the gate-voltage variation is to change the number of propagating modes supported by the quantum-point-contact leads. As the number of these modes is increased, the hybridization should become increasingly resolved, with direct consequences for the frequency content of the magnetoconductance fluctuations. Specifically, when a magnetic-field variation is used to sweep this dense density of states past the Fermi level, rapid oscillations should be observed in the conductance. Reduction of the interdot coupling should quench the hybridization, however, resulting in a sparser level spectrum and an associated suppression of high-frequency features in the magnetoconductance. It is exactly this coupling-driven transition from multiple to single-dot interference that we believe we observe in our experiment.

While the influence of varying the interdot coupling may be discussed in terms of energy hybridization, it should also be possible to provide an *equivalent* semiclassical description of this effect. In this regard, we recall that high-frequency features in the magnetoconductance are generally thought to be associated with semiclassical orbits that enclose large areas within the device. According to this interpretation, the steady reduction in the high-frequency content of the fluctuations suggests that the effect of reducing the interdot coupling is to suppress the contribution to interference of orbits that *coherently* span multiple dots of the array. Since these *global* orbits are the very ones that should give rise to hybridization of the energy spectrum, we believe that this semiclassical interpretation is quite consistent with the arguments given in the preceding paragraph. Whether we chose to discuss this effect in terms of energy hybridization, or the contribution of semiclassical orbits, however, the important feature of the studies presented here is that they reveal a nontrivial scaling of the interference in open dot arrays. In particular, we have seen that, when a number of dots are coupled to each other, the frequency content of the resulting fluctuations is not simply determined by the total area

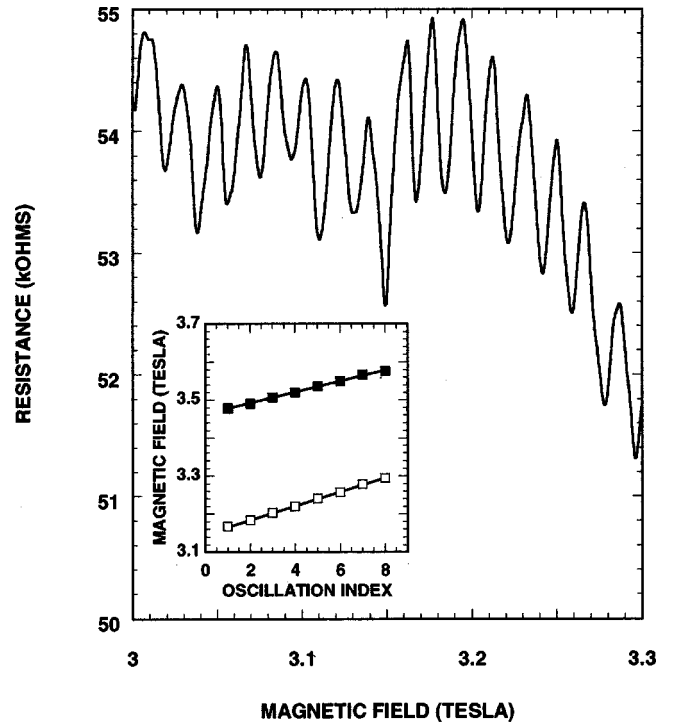


FIG. 7. Main panel: Aharonov-Bohm oscillations measured at 0.01 K in the three-dot array with lithographic dot dimensions of $0.6 \times 1.0 \mu\text{m}^2$. The applied gate voltage is -1.9 V. Inset: Variation of the magnetic-field position of successive oscillation minima with oscillation index. The open squares were obtained for a gate voltage of -1.9 V, while the filled ones were obtained for a gate voltage of -0.6 V. The solid lines represent the best linear fits to the data.

of the array, but is critically influenced by the details of the interdot coupling.

To conclusively demonstrate that the behavior observed in experiment does indeed result from a change in the coupling strength between the dots, it is necessary to rule out other, more trivial, possibilities. In particular, it might be argued that the behavior observed in Figs. 2 and 3 simply results from a gate-voltage-induced squeezing of the total area of the arrays. From the observation of Aharonov-Bohm oscillations in the high-field magnetoconductance, we exclude such a possibility, however. In the main panel of Fig. 7, we show examples of these oscillations, which were obtained for the most negative voltage applied to the gates (-1.9 V). In the inset to Fig. 7, we plot the magnetic-field position of successive oscillations as open squares and, from the slope of the resulting straight line, obtain an average oscillation period of 18.5 mT. The solid squares in this inset show the results of a similar analysis, performed for the oscillations observed with the least-negative voltage applied to the gates (-0.6 V). The period here is 14.5 mT, and from the change in oscillation period with gate voltage we infer an associated variation of roughly 20% in the effective area of the arrays. This finding is in good agreement with the results of our self-consistent potential-profile simulations, which show little variation in the effective size of the array over the gate-voltage range for which the dramatic changes in the frequency content of the fluctuations occur. Further evidence that the behavior we dis-

cuss does indeed result from the role of the interdot coupling is provided by our studies of single dots. This can be seen, for example, in the lower panel of Fig. 3, in which we show the Fourier contour obtained in studies of a single dot. Clearly, the frequency components of its fluctuations do not depend sensitively on gate voltage, a behavior very different from that found in the arrays.

An important issue we have not discussed so far concerns the range of coupling strength for which the transition between the single- and multiple dot regimes occurs. According to our experiments, the transition occurs while the arrays remain open, a finding that is confirmed by the results of the numerical studies. For the two gate voltages shown in Fig. 6, the point contacts support five (-0.6 V) and three (-0.9 V) propagating modes, for which the numbers for the average conductance of the array are 4 and $2e^2/h$, respectively. Such a variation is consistent with the results of experiment, in which the average conductance ranges from $7-2 e^2/h$ and $4-1 e^2/h$, in the upper and center panels of Fig. 3, respectively. Note in Fig. 3 that, on the right-hand side of the contour plots, we show the change in the average conductance to which the gate-voltage variation gives rise. For the data plotted in the center panel, this variation is smaller than that in the upper panel, which might account for the less dramatic evolution of the frequency content seen in the center panel. We actually expect that the characteristic coupling strength for which the transition in interference occurs should depend on the degree of decoherence in the arrays, with stronger coupling required to resolve the multiple dot behavior as the phase-breaking time is decreased. In the future, it will therefore be of interest to study the influence of temperature on the interference characteristics of the arrays. In the ultimate limit of infinite dephasing time, one would expect to observe sharp conductance resonances, whose line shape reflects the lifetime of different quasibound states in the array. While this regime cannot be accessed in mesoscopic experiments, it should be possible to perform analog studies using coupled microwave cavities, which are generally less susceptible to decoherence.²⁸

Finally, we consider the connection of this work to previous studies of molecular states in *tunnel-coupled* quantum dots.¹⁸⁻²³ In these experiments, the strength of the interdot

coupling is varied, while maintaining tunnel coupling between the dots and their charge reservoirs. The relevant experimental probe is the Coulomb oscillations in the conductance, which are washed out once the dot system is opened to its external reservoirs. This does *not* imply, however, that the hybridization is washed out at the same time. We point here to previous studies of transport in open dots, which have revealed that opening the dot to external reservoirs gives rise to a *nonuniform* broadening of its discrete states.^{8,12-15} Dependent on their coupling strength to the leads,¹⁵ certain states of the open structure survive to give rise to measurable magnetotransport results.¹³ Given this robust nature of the dot spectrum, it does not seem surprising that we are able to observe features due to hybridization of its states in the open arrays that we study. Indeed, such a possibility was even suggested in an earlier theoretical study.¹⁷ It is also interesting to note that, in studies of tunnel-coupled dots, evidence for hybridization is found in situations where the coupling between the component dots is provided by tunnel barriers.¹⁹⁻²³ In contrast, the transition to single-dot behavior reported here clearly occurs while the point-contact leads that couple the dots support several modes. The situation in our experiments is quite different to that in the tunnel-coupled dots, however, since in our case we vary the dot-dot and dot-reservoir coupling strengths *simultaneously*.

In conclusion, the magnetoconductance fluctuations in open quantum-dot arrays have been found to exhibit evidence for a transition from multiple to single-dot interference that occurs as the strength of the interdot coupling is varied. These results therefore reveal a nontrivial scaling of the conductance fluctuations in the arrays, which is thought to arise from the influence of the interdot coupling on energy hybridization. In an equivalent semiclassical description, the change in the frequency content of the fluctuations is thought to result from a suppression of the contribution to coherent interference from global orbits, which span multiple dots of the array. Support for these arguments is provided by the absence of such behavior in equivalent experiments performed on single dots, and by the results of realistic numerical simulations.

This work was supported by the Office of Naval Research and by the NSF/JSPPS.

¹R. A. Jalabert, H. U. Baranger, and A. D. Stone, Phys. Rev. Lett. **65**, 2442 (1990).

²C. M. Marcus, A. J. Rimberg, R. M. Westervelt, P. F. Hopkins, and A. C. Gossard, Phys. Rev. Lett. **69**, 506 (1992).

³A. M. Chang, H. U. Baranger, L. N. Pfeiffer, and K. W. West, Phys. Rev. Lett. **73**, 2111 (1994).

⁴I. H. Chan, R. M. Clarke, C. M. Marcus, K. Campman, and A. C. Gossard, Phys. Rev. Lett. **74**, 3876 (1995).

⁵M. Persson, J. Pettersson, B. von Sydow, P. E. Lindelof, A. Kristensen, and K.-F. Berggren, Phys. Rev. B **52**, 8921 (1995).

⁶J. P. Bird, J. Phys.: Condens. Matter **11**, R413 (1999).

⁷R. Akis, D. K. Ferry, and J. P. Bird, Phys. Rev. Lett. **79**, 123 (1997).

⁸I. V. Zozoulenko, R. Schuster, K. F. Berggren, and K. Ensslin, Phys. Rev. B **55**, R10 209 (1997).

⁹R. P. Taylor, R. Newbury, A. S. Sachrajda, Y. Feng, P. T. Coleridge, C. Dettmann, N. Zhu, H. Guo, A. Delage, P. J. Kelly, and Z. Wasilewski, Phys. Rev. Lett. **78**, 1952 (1997).

¹⁰A. S. Sachrajda, R. Ketzmerick, C. Gould, Y. Feng, P. J. Kelly, A. Delage, and Z. Wasilewski, Phys. Rev. Lett. **80**, 1948 (1998).

¹¹D. P. Pivin, Jr., A. Andresen, J. P. Bird, and D. K. Ferry, Phys. Rev. Lett. **82**, 4687 (1999).

¹²J. P. Bird, R. Akis, D. K. Ferry, D. Vasileska, J. Cooper, Y. Aoyagi, and T. Sugano, Phys. Rev. Lett. **82**, 4691 (1999).

¹³J. P. Bird, R. Akis, and D. K. Ferry, Phys. Rev. B **60**, 13 676 (1999).

- ¹⁴I. V. Zozoulenko, A. S. Sachrajda, C. Gould, K.-F. Berggren, P. Zawadzki, Y. Feng, and Z. Wasilewski, *Phys. Rev. Lett.* **83**, 1838 (1999).
- ¹⁵R. Akis, J. P. Bird, D. K. Ferry, and D. Vasileska, *Physica E (Amsterdam)* **7**, 745 (2000).
- ¹⁶J. P. Bird, A. P. Micolich, H. Linke, D. K. Ferry, R. Akis, Y. Ochiai, Y. Aoyagi, and T. Sugano, *J. Phys.: Condens. Matter* **10**, L55 (1998).
- ¹⁷R. Akis and D. K. Ferry, *Phys. Rev. B* **59**, 7529 (1999).
- ¹⁸L. P. Kouwenhoven, F. W. J. Hekking, B. J. van Wees, C. J. P. M. Harmans, C. E. Timmering, and C. T. Foxon, *Phys. Rev. Lett.* **65**, 361 (1990).
- ¹⁹F. R. Waugh, M. J. Berry, D. J. Mar, R. M. Westervelt, K. L. Campman, and A. C. Gossard, *Phys. Rev. Lett.* **75**, 705 (1995).
- ²⁰T. H. Oosterkamp, T. Fujisawa, W. G. van der Wiel, K. Ishibashi, R. V. Hijman, S. Tarucha, and L. P. Kouwenhoven, *Nature (London)* **395**, 873 (1998).
- ²¹T. Fujisawa, T. H. Oosterkamp, W. G. van der Wiel, B. W. Broer, R. Aguado, S. Tarucha, and L. P. Kouwenhoven, *Science* **282**, 932 (1998).
- ²²R. H. Blick, D. W. van der Weide, R. J. Haug, and K. von Klitzing, *Phys. Rev. Lett.* **81**, 689 (1998).
- ²³R. H. Blick, D. Pfannkuche, R. J. Haug, K. v. Klitzing, and K. Eberl, *Phys. Rev. Lett.* **80**, 4032 (1998).
- ²⁴J. P. Bird, A. Shailos, M. Elhassan, C. Prasad, D. K. Ferry, L.-H. Lin, N. Aoki, Y. Ochiai, K. Ishibashi, and Y. Aoyagi, *Nanotechnology* **11**, 365 (2000).
- ²⁵L. Christensson, H. Linke, P. Omling, P. E. Lindelof, I. V. Zozoulenko, and K.-F. Berggren, *Phys. Rev. B* **57**, 12 306 (1998).
- ²⁶R. Akis, J. P. Bird, and D. K. Ferry, *Phys. Condens. Matter* **8**, L667 (1996).
- ²⁷R. Akis, D. K. Ferry, and J. P. Bird, *Phys. Rev. B* **54**, 17 705 (1996).
- ²⁸H.-J. Stöckmann, *Quantum Chaos: An Introduction* (Cambridge University Press, Cambridge, England, 1999).